Isospinning hopfions

Derek Harland[1], Juha Jäykkä[2], Martin Speight[3] and Yakov Shnir[3]

[1]Department of Mathematical Sciences, Loughborough University
Loughborough LE11 3TU, England

[2]Nordita, KTH Royal Institute of Technology and Stockholm University
Roslagstullsbacken 23, SE-106 91 Stockholm, Sweden

[3]School of Mathematics, University of Leeds
Leeds LS2 9JT, England

Abstract

The problem of constructing internally rotating solitons of fixed angular frequency ω in the Faddeev-Skyrme model is reformulated as a variational problem for an energy-like functional, called pseudoenergy, which depends parametrically on ω. This problem is solved numerically using a gradient descent method, without imposing any spatial symmetries on the solitons, and the dependence of the solitons' energy on ω, and on their conserved total isospin J, studied. It is found that, generically, the shape of a soliton is independent of ω, and that its size grows monotonically with ω. A simple elastic rod model of time-dependent hopfions is developed which, despite having only one free parameter, accounts well for most of the numerical results.

PACS classification numbers: 05.45.Yv, 03.50.-z
Keywords: topological solitons, knot solitons

1 Introduction

Many field theories of interest in fundamental physics support topological solitons – spatially localized, stable lumps of energy whose strongly particle-like characteristics make them natural theoretical models of elementary particles. Perhaps the best developed model from this viewpoint is the Skyrme model, whose solitons are posited to model atomic nuclei. It is of fundamental importance in this context that individual solitons possess both rotational and internal rotational (or *isorotational*) degrees of freedom. In the Skyrme model, the rotational degrees of freedom account, after quantization, for the spin of atomic nuclei, while the isorotational degrees of freedom account, roughly speaking, for their difference in "flavour". For example, both protons and neutrons are modelled by degree one solitons, the only difference being in the sense in which they are (internally) spinning. In practice, finding even

static classical solitons is a significant computational challenge, so it is not surprising that almost all studies of (iso)spinning solitons work within a rigid body type approximation: the (iso)spinning soliton is assumed to have precisely the same shape as the static soliton, but with its spatial and internal orientation allowed to vary in time [2, 10]. It has long been recognized that this is not a very satisfactory approximation, and various attempts have been made to improve on it [14, 11]. With a few exceptions [1, 3], these have fallen short of numerically solving the full field equations to construct genuine (iso)spinning solutions.

In this paper we construct genuine isospinning (i.e. internally rotating) soliton solutions in the Faddeev-Skyrme model [4]. Such solitons are conventionally called hopfions, since they are classified topologically by their Hopf degree (an integer-valued topological invariant). Explicitly, our field φ is S^2 valued, lives in $\mathbb{R}^{3+1}$, and has Lagrangian density

$$\mathcal{L} = \frac{1}{2}\partial_\mu\varphi \cdot \partial^\mu\varphi - \frac{1}{4}(\partial_\mu\varphi \times \partial_\nu\varphi) \cdot (\partial^\mu\varphi \times \partial^\nu\varphi) - \frac{1}{2}\mu^2(1-\varphi_3^2). \tag{1.1}$$

This model is ideal for our purposes because it is three-dimensional and has a rather rich spectrum of static soliton solutions, which should be understood as (possibly linked or self-knotted) string-like objects, but has only one internal rotational degree of freedom, because the potential breaks the internal rotational symmetry group to $SO(2)$. (Of course, one needs a potential term in $\mathcal{L}$ in order to allow any isospinning solutions at all.) Hence one can ask unambiguously "what is the degree Q isospinning hopfion of given angular frequency $\omega \in \mathbb{R}$?" For a given degree Q, there are usually several different stable static soliton solutions of rather similar energy (the number of solutions seems to grow with Q; see [5] for a study of static hopfions in a model with potential). It is interesting to discover how the energy of such solitons varies as their angular frequency (or their conserved isospin) changes. We will find several examples where these energy curves cross, so that the most energetically favourable shape of the hopfion for a given degree Q changes when one isospins them fast enough.

Our method is to use the Principle of Symmetric Criticality to reduce the problem of finding isospinning solitons of angular frequency ω to a static "energy" minimization problem, where the "energy" to be minimized (more properly called pseudo-energy) F_ω depends parametrically on ω. We solve this problem numerically by a standard gradient descent method. Starting at $\omega = 0$ (where the solitons are already well understood), we gradually increment ω and reminimize, in this way constructing curves of isospinning solitons, parametrized by ω. This method allows us to construct isospinning solitons without imposing axial symmetry, in contrast to previous studies which have used simulated annealing [3] or direct solution of the field equations [1]. Since very few static Hopf solitons are axially symmetric, this is a significant advantage.

We expect that at least one minimizer of F_ω exists for each Q whilever $\omega < \min\{\omega_1, \omega_2\}$, where ω_1 is determined by the radius of the target two-sphere (here taken to be 1) and $\omega_2 = \mu$ is determined by the "meson" mass of the model. In fact, one could prove this, at least for Q in an infinite (but unknown) subset of $\mathbb{Z}$, by an obvious modification of the methods of Lin and Yang [12], who considered the functional F_0 with $\mu = 0$. It is well understood that solitons cannot spin with $\omega > \mu$ because they become unstable to radiation of mesons. We will see evidence, however, that if $\mu > 1$, solitons generically lose stability and collapse *before* ω reaches μ, due to the extra nonlinear velocity dependence generated by the Skyrme term. This is not specific to the model considered here, and should be generic for Skyrme-type models.

We are able to get significant analytic insight into the behaviour of isospinning hopfions by developing a time-dependent extension of the elastic rod model of hopfions introduced recently by two of us, in collaboration with Sutcliffe [7]. This extended model, which is of considerable geometric interest in its own right, predicts a universal energy-frequency relationship, in rather good agreement with our main numerical results. We also test the rod model by comparing its predictions for infinite isospinning Hopf strings (i.e. solutions which are equivariant with respect to translations in a fixed direction) with numerics. Again, we find rather good agreement.

The rest of this paper is structured as follows. In section 2 we reduce the problem of finding isospinning hopfions to an energy minimization problem. In section 3 we develop an elastic rod model for time-dependent Faddeev-Skyrme fields and extract phenomenolgical predictions on isospinning hopfions and Hopf strings. In section 4 we present our numerical results, which are briefly summarized in section 5.

2 Reduction to a static variational problem

Since isorotation involves only rotational symmetry of the target space S^2, it is convenient to consider the Faddeev-Skyrme model on a general oriented Riemannian manifold M. This allows one to treat in unified fashion the case of principal interest, $M = \mathbb{R}^3$, and the cases of soliton chains or strings, $M = \mathbb{R}^2 \times S^1$, sheets $M = \mathbb{R} \times T^2$, or geometrically nontrivial domains (of potential interest for cosmological applications, for example). Given a time-dependent field $\varphi : \mathbb{R} \times M \to S^2$, we have at each fixed time t a mapping $\varphi(t, \cdot) : M \to S^2$ which we shall, in a slight abuse of notation, again denote φ, and a time derivative $\dot{\varphi}$, which is a section of the bundle $\varphi^{-1}TS^2$ over M. Using these, we define, at time t, the kinetic and potential energy functionals to be

$$T = \int_M \frac{1}{2}|\dot{\varphi}|^2 + \frac{1}{2}|\varphi^*(\iota_{\dot{\varphi}}\Omega)|^2 \tag{2.1}$$

$$V = \int_M \frac{1}{2}|\mathrm{d}\varphi|^2 + \frac{1}{2}|\varphi^*\Omega|^2 + U(\varphi), \tag{2.2}$$

where Ω is the area form on S^2, $\varphi^*\Omega$ its pullback to M, ι denotes interior product, and $U : S^2 \to [0, \infty)$ is a smooth potential function which we assume attains its minimum value 0 at some point $\psi_\infty \in S^2$, and is invariant under rotations about ψ_∞. If M is noncompact, we assume that $\varphi(t, x) \to \psi_\infty$, as $x \to \partial_\infty M$, sufficiently fast for all integrals to converge.

Let $\omega > 0$ be a fixed constant. We seek time-periodic solutions of period $2\pi/\omega$. By definition, these are critical points $\varphi : S^1_\omega \times M \to S^2$ of the action functional

$$S(\varphi) = \int_{S^1_\omega} (T - V) \tag{2.3}$$

where $S^1_\omega = \mathbb{R}/(2\pi/\omega)\mathbb{Z}$ is the circle of length $2\pi/\omega$. Denote by X_ω the completion in C^1 of the set of smooth maps $\varphi : S^1_\omega \times M \to S^2$ of finite action. We define an action of the group $S^1 = \mathbb{R}/2\pi\mathbb{Z}$ on X_ω as follows:

$$([\alpha], \varphi) \mapsto \varphi_{[\alpha]}, \qquad \varphi_{[\alpha]}(t, x) = R(\alpha)\varphi(t - \alpha/\omega, x) \tag{2.4}$$

where $R(\alpha)$ denotes the $SO(3)$ matrix generating rotation through angle α about the axis ψ_∞. Clearly, $S(\varphi_{[\alpha]}) = S(\varphi)$ for all $([\alpha], \varphi)$, since the action is separately invariant under both time translation and isorotation about ψ_∞. Denote by $X_\omega^{S^1}$ the set of fixed points of this action. Then $\varphi \in X_\omega^{S^1}$ if and only if

$$\varphi(t, x) = R(\omega t)\psi(x) \tag{2.5}$$

for some map $\psi : M \to S^2$. We may think of ψ as the stationary field φ when viewed in an internally corotating frame. Since S^1 is compact, it follows from the Principle of Symmetric Criticality [13] that $\varphi \in X_\omega^{S^1}$ is a critical point of $S : X_\omega \to \mathbb{R}$ if and only if it is a critical point of the restricted action $S : X_\omega^{S^1} \to \mathbb{R}$. Now

$$S(R(\omega t)\psi(x)) = \frac{2\pi}{\omega}\left\{\frac{1}{2}\omega^2 \int_M (|\psi_\infty \times \psi|^2 + |\mathrm{d}(\psi_\infty \cdot \psi)|^2) - V(\psi)\right\}, \tag{2.6}$$

so a uniformly isorotating field of the form (2.5) is a critical point of S if and only if the static field $\psi : M \to S^2$ is a critical point of the functional

$$F_\omega(\psi) = \int_M \left\{\frac{1}{2}(|\mathrm{d}\psi|^2 - \omega^2|\mathrm{d}(\psi_\infty \cdot \psi)|^2) + \frac{1}{2}|\psi^*\Omega|^2 + (U(\psi) - \frac{1}{2}\omega^2|\psi_\infty \times \psi|^2)\right\}. \tag{2.7}$$

We shall call this functional the *pseudoenergy* of ψ. It has a rather interesting and natural form, as we now describe.

The first two terms of (2.7), taken together, can be interpreted as the Dirichlet energy of the map $\psi : M \to S^2$, where S^2 is given the deformed metric

$$\langle X, Y\rangle_\omega = X \cdot Y - \omega^2(\psi_\infty \cdot X)(\psi_\infty \cdot Y) \tag{2.8}$$

for all $X, Y \in T_\psi S^2$. For $0 < \omega < 1$ this metric gives S^2 the geometry of an oblate sphere, squashed along the direction of ψ_∞. For $\omega > 1$, the metric is singular, changing from Riemannian to Lorentzian in a strip around the equator (orthogonal to ψ_∞). Consequently, the pseudoenergy F_ω is no longer bounded below for $\omega > \omega_1 = 1$ which, as we will see, has strong phenomenological consequences.

The third term of F_ω is just the usual Faddeev-Skyrme term (quartic in spatial derivatives). The fourth and fifth terms together can be interpreted as a deformed potential

$$U_\omega(\psi) = U(\psi) - \frac{1}{2}\omega^2|\psi_\infty \times \psi|^2. \tag{2.9}$$

Since U attains its minimum at ψ_∞ and is rotationally invariant, its hessian about ψ_∞ must be $\mu^2\langle\cdot,\cdot\rangle$ for some constant $\mu \geq 0$, interpreted physically as the mass of mesons in the field theory. Hence, if $\omega > \omega_2 = \mu$, F_ω is again unbounded below. A particularly convenient choice for U is

$$U(\psi) = \frac{1}{2}\mu^2(1 - \psi_3^2)^2. \tag{2.10}$$

Then $\psi_\infty = (0, 0, 1)$ and the deformed potential is

$$U_\omega(\psi) = \frac{1}{2}(\mu^2 - \omega^2)(1 - \psi_3^2)^2. \tag{2.11}$$

This is the potential we use in all our numerical simulations.

Since the model is invariant under global rotations of φ about ψ_∞, it has an associated conserved Noether charge, called *isospin*

$$J = \int_M \{\dot{\varphi} \cdot (\psi_\infty \times \varphi) + \langle \mathrm{d}(\psi_\infty \cdot \varphi), \varphi^*(\iota_{\dot{\varphi}}\Omega)\rangle\}\,. \tag{2.12}$$

For uniformly isorotating fields of the form (2.5), this equals

$$J = \Lambda(\psi)\omega \tag{2.13}$$

where the moment of inertia is

$$\Lambda(\psi) = \int_M \left\{|\psi_\infty \times \psi|^2 + |\mathrm{d}(\psi_\infty \cdot \psi)|^2\right\}. \tag{2.14}$$

Hence $F_\omega(\psi) = V(\psi) - \frac{1}{2}\omega^2\Lambda(\psi)$, while the total energy of the field (2.5) is $V + T = V(\psi) + J^2/(2\Lambda(\psi))$. There are two natural variational problems for ψ:

1. For fixed ω, extremize $F_\omega(\psi) = V(\psi) - \frac{1}{2}\omega^2\Lambda(\psi)$;
2. For fixed J, extremize $E_J(\psi) = V(\psi) + J^2/(2\Lambda(\psi))$.

It is clear that these two problems are precisely equivalent: if ψ solves 1, then it solves 2 with $J = \Lambda(\psi)\omega$, and if ψ' solves 2, it solves 1 with $\omega = J/\Lambda(\psi')$. Previous studies [3] of isorotating[1] solitons have used formulation 2, whereas in this paper we will mainly use formulation 1. This has several advantages. First, it is directly clear, as we have shown (using the Principle of Symmetric Criticality), that solutions of 1 correspond via (2.5) to genuine solutions of the field theory. Second, the Euler-Lagrange equation corresponding to 1 is a PDE, similar in structure to the static field equation of the Faddeev-Skyrme model, whereas the equation corresponding to 2 is a rather more complicated differential-integral equation. Consequently, it is a fairly simple matter to adapt existing numerical techniques, developed for the static FS model, to deal with problem 1. Third, formulation 1 makes it clear that, in the case $\mu > 1$, there is no reason why isospinning solitons should persist for frequencies $\omega \in (1, \mu)$, since F_ω is unbounded below when $\omega > \min\{1, \mu\}$. Hence, we have the possibility that isospinning hopfions are destabilized by nonlinear velocity terms in the field equation *before* they reach the upper limit $\omega = \mu$.

To conclude this section, we note that a general time dependent solution of the model $\varphi(t, x) = R(\omega t)\psi(t, x)$ conserves both total energy $T + V$ and isospin J, and hence conserves

$$T + V - \omega J = F_\omega(\psi) + \frac{1}{2}\int_M (|\dot{\psi}|^2 + |\iota_{\dot{\psi}}\Omega|^2). \tag{2.15}$$

Hence a local minimum of $F_\omega(\psi)$ corresponds to an orbitally stable solution of the model, since a small perturbation of ψ is trapped close to ψ by conservation of $T + V - \omega J$. So the solutions found by our numerical method, which can only find minima of F_ω, are guaranteed to be orbitally stable. One should note that conservation of $T + V - \omega J$ does not directly imply that saddle points of F_ω are unstable.

[1] Actually, [3] concerns spatially rotating Skyrmions, but within the axially symmetric ansatz used therein, rotation is equivalent to isorotation.

3 An elastic rod model

Before embarking on numerical investigation of the variational problems posed in the previous section, it is useful to consider analogous problems in a simple effective model of Faddeev-Skyrme solitons. A model based on elastic rods was introduced in [7], which successfully captures the qualitative features of static solitons with small Hopf degree on both $M = \mathbb{R}^3$ [7] and $M = \mathbb{R}^2 \times S^1$ [6]. Although originally formulated only in flat 3-space, the model has a geometrically natural extension to any curved Lorentzian 4-manifold representing space-time, allowing one to model time-dependent solitons.

The degrees of freedom in the elastic rod model consist of a smooth map x from an oriented 2-manifold Σ into a 4-manifold $\mathcal{M}$ equipped with a Lorentzian metric g, and a section m of the normal bundle $N\Sigma$ of unit length. The image of x is taken to represent the preimage under φ of the point $-\psi_\infty$ in S^2 antipodal to ψ_∞, and the section m represents the projection onto $N\Sigma$ of the pull-back under φ of a fixed vector in the tangent space at $-\psi_\infty$. The SO(2) internal symmetry group of the Faddeev-Skyrme model, which rotates the target 2-sphere leaving ψ_∞ fixed, can be identified with the SO(2) structure group of $N\Sigma$. The latter acts naturally on m, since the sphere bundle and the bundle of linear frames for $N\Sigma$ can be identified.

The elastic rod model is defined by an action comprising three terms which describe the effects of stretching, bending, and twisting of the rod. The stretching term S_S is simply the area of Σ, as measured using the metric γ on Σ induced from g:

$$S_S(x) := -\int_\Sigma Vol_\gamma. \tag{3.1}$$

This is nothing other than the Nambu-Goto action of string theory.

The bending term S_B is constructed from the second fundamental form $\mathbb{I}$ of Σ. The latter is a section of $\mathrm{Sym}^2(T^*\Sigma) \otimes N\Sigma$ and is defined by the equation,

$$\mathbb{I}(X, Y) = \pi_N(\nabla^{LC}_X Y) \quad \forall X, Y \in \Gamma(T\Sigma). \tag{3.2}$$

Here ∇^{LC} denotes the pull-back of the Levi-Civita connexion on $\mathcal{M}$ to $x^*(T\mathcal{M})$ and π_N denotes the orthogonal projection from $x^*(T\mathcal{M})$ to $N\Sigma$. Since there are two naturally defined quadratic forms on $\mathrm{Sym}^2(T^*\Sigma)$, there are two ways to build an action from $\mathbb{I}$. Introducing coordinates σ^a on Σ and y^μ on $\mathcal{M}$, the two possible actions built from $\mathbb{I} = \mathbb{I}^\mu_{ab} \mathrm{d}\sigma^a \mathrm{d}\sigma^b \partial_\mu$ are:

$$S_B(x) := \int_\Sigma g_{\mu\nu} \gamma^{ab} \gamma^{cd} \mathbb{I}^\mu_{ab} \mathbb{I}^\nu_{cd} Vol_\gamma \quad \text{and} \quad S'_B(x) := \int_\Sigma g_{\mu\nu} \gamma^{ab} \gamma^{cd} \mathbb{I}^\mu_{da} \mathbb{I}^\nu_{bc} Vol_\gamma. \tag{3.3}$$

These correspond to taking either the square of the trace or the trace of the square of the second fundamental form.

While in general one should consider actions involving both terms S_B and S'_B, in applications in which $\mathcal{M}$ is flat one may work solely with S_B without any loss of generality. The reason is that in this situation the equations of motion for both terms agree, as we now prove. Suppose that the Riemann curvature tensor for $\mathcal{M}$ vanishes. Then the Riemannian curvature R of γ may be expressed in terms of the second fundamental form using Gauss's formula:

$$R_{abcd} = g_{\mu\nu}(\mathbb{I}^\mu_{ac} \mathbb{I}^\nu_{bd} - \mathbb{I}^\mu_{ad} \mathbb{I}^\nu_{bc}). \tag{3.4}$$

Contracting with $\gamma^{ac}\gamma^{bd}$ and integrating over Σ results in the equation,

$$\int_\Sigma Sc\ Vol_\gamma = S_B - S'_B, \tag{3.5}$$

in which Sc denotes the scalar curvature of γ. The left hand side of this equation is equal to a linear combination of the Euler characteristic of Σ and an integral over the boundary of Σ, by the Gauss-Bonnet theorem for manifolds with indefinite signature [9]. In particular, it is stable to small local perturbations of x and thus has a trivial Euler-Lagrange equation. Therefore the Euler-Lagrange equations for S_B and S'_B coincide.

The twisting term S_T is built from the derivatives of m. Recall that a connexion ∇^N can be defined on the normal bundle $N\Sigma$ by orthogonally projecting the Levi-Civita connexion on $x^*T\mathcal{M}$:

$$\nabla^N_X m := \pi^N \nabla^{LC}_X m \quad \forall X \in T\Sigma, m \in N\Sigma. \tag{3.6}$$

The twist rate θ associated to the unit normal vector m is the projection of the covariant derivative of m to the subspace of $N\Sigma$ orthogonal to m. More precisely, θ is a section of $T^*\Sigma$ defined by the equation

$$\theta(X) Vol_\gamma(Y,Z) = Vol_g(\nabla_X m, m, Y, Z) \quad \forall X, Y, Z \in \Gamma(T\Sigma). \tag{3.7}$$

The twisting term is then

$$S_T(x,m) := \int_\Sigma \gamma^{ab}\theta_a\theta_b Vol_\gamma = \int_\Sigma \theta \wedge *_\gamma \theta. \tag{3.8}$$

Equivalently, the twisting term may defined to be the L^2 norm of $\nabla^N m$.

The complete action for the elastic rod model takes the form

$$S(x,m) = AS_S(x) + BS_B(x) + CS_T(x,m), \tag{3.9}$$

with A, B, C positive real parameters. Of these, two correspond to choices of units while only the dimensionless ratio B/C is non-trivial.

3.1 Isospinning rods

From now on the target manifold $\mathcal{M}$ is taken to be $\mathbb{R}^3 \times S^1_\omega$ equipped with its standard Lorentzian metric, and Σ is taken to be compact. Let Y_ω denote the set of C^2 pairs (x,m) consisting of an immersion $x : \Sigma \to \mathcal{M}$ and a section m of $N\Sigma \subset x^{-1}T\mathcal{M}$. For each m denote by m' the unique section of $N\Sigma$ such that m, m' is a positively oriented orthonormal basis, and let $K_{[\alpha]}$ denote the action of translation along S^1_ω by α/ω on $\mathbb{R}^3 \times S^1_\omega$. The action of S^1 on Y_ω corresponding to the action on X_ω is given by

$$(x,m,\alpha) \mapsto (x_{[\alpha]}, m_{[\alpha]}), \quad x_{[\alpha]} := K_{[\alpha]} \circ x, \quad m_{[\alpha]} := m\cos\alpha + m' \sin\alpha. \tag{3.10}$$

The set of fixed points of this action will be denoted $Y^{S^1}_\omega$, and elements of this set may be described as follows. Let Υ be a compact 1-manifold, let $\mathbf{x} : \Upsilon \to \mathbb{R}^3$, and let $\mathbf{m}(s)$ be a unit

vector perpendicular to $\partial_s \mathbf{x}$. Suppose that a local coordinate s on Υ has been chosen so that $|\partial_s \mathbf{x}| = 1$; then the map is said to be arclength parametrised. Any element of $Y_\omega^{S^1}$ takes the form

$$\begin{aligned} \Sigma &= S^1_\omega \times \Upsilon & (3.11)\\ x(t,s) &= (t, \mathbf{x}(s)) & (3.12)\\ m(t,s) &= \cos\omega t\, \mathbf{m}(s) + \sin\omega t\, \mathbf{t}(s) \times \mathbf{m}(s) & (3.13) \end{aligned}$$

for some $\Upsilon, \mathbf{x}, \mathbf{m}$.

Recall that in the standard Frenet formalism for curves the unit tangent vector is defined to be $\mathbf{t}(s) := \partial_s \mathbf{x}(s)$, and the curvature is $\kappa(s) := |\partial_s \mathbf{t}|$. The action for an element of $Y_\omega^{S^1}$ is $S = -(2\pi/\omega)F_\omega$, where

$$F_\omega(\Upsilon, \mathbf{x}, \mathbf{m}) := \int_\Upsilon \left(A - C\omega^2 + B\kappa^2 + C(\mathbf{t}\cdot\partial_s\mathbf{m}\times\mathbf{m})^2\right) \mathrm{d}s. \tag{3.14}$$

The critical points of the restriction of F_ω to $Y_\omega^{S^1}$ are critical points of S within Y_ω by the Principle of Symmetric Criticality [13].

As in the Faddeev-Skyrme model, the pseudoenergy for the rod model is bounded from below only for a range of values of ω. Thus F_ω can only reasonably be expected to have critical points if $\omega^2 \leq A/C$, and attention will be restricted to this range.

A crucial property of F_ω, which underpins the subsequent analysis, is that F_ω is equivalent to F_0 up to a rescaling of lengths and energies:

$$F_\omega(\Upsilon, \mathbf{x}, \mathbf{m}) = \sqrt{1-\omega^2 C/A}\, F_0\left(\Upsilon, \sqrt{1-\omega^2 C/A}\,\mathbf{x}, \mathbf{m}\right). \tag{3.15}$$

This means that properties of F_ω and its critical points can be gleaned directly from properties of F_0 with no extra effort, in contrast with the full Faddeev-Skyrme model.

Within the elastic rod model there is a conserved energy E and a conserved isospin $J = -2C\int_\Upsilon *\theta$ which are the Noether charges associated with the symmetries of time translation and rotation of $\mathbf{m}$. For elements of $Y_\omega^{S^1}$ these take the form $E_J = V + J^2/2\Lambda$ and $J = \omega\Lambda$, with

$$\begin{aligned} V &= \int_\Upsilon \left(A + B\kappa^2 + C(\mathbf{t}\cdot\partial_s\mathbf{m}\times\mathbf{m})^2\right)\mathrm{d}s \quad \text{and} & (3.16)\\ \Lambda &= \int_\Upsilon 2C\mathrm{d}s. & (3.17) \end{aligned}$$

In particular, V is the energy functional for rods introduced in [7] (to see this, note that if $\mathbf{m} = \sin\alpha(s)\mathbf{n} + \cos\alpha(s)\mathbf{b}$ then $\mathbf{t}\cdot\partial_s\mathbf{m}\times\mathbf{m} = \partial_s\alpha - \tau$ with τ denoting the torsion).

Previous studies [7, 6] have found that the static rod model defined by V provides a useful approximation to Skyrme-Faddeev solitons if a value of approximately 0.85 is chosen for the dimensionless ratio C/B. The same choice should be equally useful in the Faddeev-Skyrme model with $U \neq 0$, since qualitative properties of solitons seem unaffected by the introduction of U [5]. In practice it is necessary to impose constraints on elastic rods in order to prevent self-intersections, but these can safely be ignored for the purposes of the present discussion.

The static rod model successfully captures qualitative features of all low-charge Faddeev-Skyrme solitons, with a minor exception at charge 4. The problem at charge 4 is that the minimal energy soliton is an $\mathcal{A}_{2,2}$ knot consisting of two superposed charge 2 solitons, and the rod model is unable to describe such a configuration. The charge 4 $\mathcal{A}_{2,2}$ soliton is the only known energy-minimising soliton which is a superposition of lower charge solitons, so this shortcoming of the rod model is very mild. Thus we expect that useful insight into the variational problems 1 and 2 posed in section 2 can be inferred by studying the corresponding problems for rods.

3.2 Infinite strings

Before considering solitons on $\mathbb{R}^3$ within the rod model, we will first discuss a simpler situtation of solitons with cylindrical symmetry. Let $P > 0$ and let us replace physical space $M = \mathbb{R}^3$ by $M = \mathbb{R}^2 \times S^1_{2\pi/P}$. The ansatz,

$$\Upsilon = S^1_{2\pi/P}, \quad \mathbf{x}(s) = (0, 0, s), \quad \mathbf{m}(s) = (\cos(2\pi s/P), \sin(2\pi s/P), 0), \tag{3.18}$$

describes the unique fixed point of a certain action of $S^1 \times \mathrm{SO}(2)$ on $Y_\omega^{S^1}$. It is a critical point of the pseudoenergy at which the potential energy and moment of inertia take the values

$$V = AP + \frac{(2\pi)^2 C}{P} \quad \text{and} \tag{3.19}$$

$$\Lambda = 2PC. \tag{3.20}$$

Consider an extension of variational problem 2, in which E_J is extremized with respect to variations in P, $\mathbf{x}$ and $\mathbf{m}$ while J is held fixed. For each J the expression $E_J = V + J^2/2\Lambda$ has a unique minimum amongst $S^1 \times \mathrm{SO}(2)$-symmetric configurations. The values $E_0(J)$, $P_0(J)$ and $\omega_0(J)$ of E, P and ω at the minimum are easily obtained from equations (3.19) and (3.20) and the expression $\omega = J/\Lambda$:

$$E_0(J) = \sqrt{(4\pi)^2 AC + \frac{A}{C} J^2} \tag{3.21}$$

$$P_0(J) = 2\pi \sqrt{\frac{C}{A} + \frac{J^2}{(4\pi)^2 AC}} \tag{3.22}$$

$$\omega_0(J) = \frac{\frac{A}{C} J}{\sqrt{(4\pi)^2 AC + \frac{A}{C} J^2}}. \tag{3.23}$$

These equations show that both $E_0(J)$ and $P_0(J)$ grow linearly with J for large values of J, and that ω is approximately constant for large values of J. They also imply that the dimensionless quantity $E_0 P_0^2 \mathrm{d}\omega_0/\mathrm{d}J$ evaluates to $4\pi^2$ at $J = 0$. These qualitative and quantitative predictions will now be tested in the Faddeev-Skyrme model.

Imposing $S^1 \times \mathrm{SO}(2)$ symmetry in the Faddeev-Skyrme model results in the following ansatz for ψ in terms of a profile function $f(r)$:

$$\psi = (\sin f(r) \cos(\theta + 2\pi z/P), \sin f(r) \sin(\theta + 2\pi z/P), \cos f(r)) \,. \tag{3.24}$$

The expressions for V and Λ are

$$V = \pi \int_0^\infty \left\{ (f')^2 + \left(\left(\frac{2\pi}{P} \right)^2 + \frac{1}{r^2} \right) \sin^2 f \left(1 + (f')^2 \right) + \mu^2 \sin^2 f \right\} r \mathrm{d}r \tag{3.25}$$

$$\Lambda = 2\pi \int_0^\infty \left(1 + (f')^2 \right) \sin^2 f \, r \mathrm{d}r. \tag{3.26}$$

The boundary conditions $f(0) = 0$ and $f(r) \to \pi$ as $r \to \infty$ are imposed in order to maintain continuity at the origin and finiteness of V and Λ.

Variational problem 2 may now be studied using the following numerical scheme. Let $V(\omega, P)$ and $\Lambda(\omega, P)$ denote the values of V and Λ at a critical point of $F_\omega = V - \frac{1}{2}\omega^2 \Lambda$. The values of the functions $V(\omega, P)$ and $\Lambda(\omega, P)$ at any pair (ω, P) may be determined by first determining a numerical solution f to the Euler-Lagrange equation associated with F_ω and then numerically evaluating the integral expressions for V and Λ. A minimum $E_0(J)$ of $E = V + \frac{1}{2}\omega^2 \Lambda$ with $J = \Lambda\omega$ held fixed can be determined by numerically solving the J-preserving gradient flow equation for E in ω and P:

$$\begin{aligned} \dot{P} &= -\partial_P E(\omega, P) + M \partial_P J(\omega, P) \\ \dot{\omega} &= -\partial_\omega E(\omega, P) + M \partial_\omega J(\omega, P) \\ M &= \frac{\partial_P E \partial_P J + \partial_\omega E \partial_\omega J}{\partial_P J \partial_P J + \partial_\omega J \partial_\omega J}. \end{aligned} \tag{3.27}$$

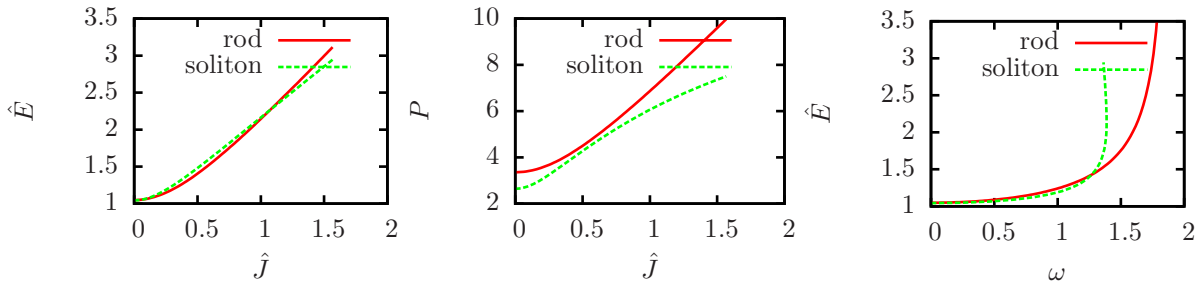

Figure 1: Infinite strings in the Faddeev-Skyrme model solving variational problem 2. The graphs show the energy E and period P as functions of the isospin, and also the energy E as a function of the parameter ω.

The results of this procedure are presented in figure 1. The numerical results confirm the three qualitative predictions derived in the rod model for large J, namely that $E_0(J)$ and $P_0(J)$ grow linearly with J, while $\omega_0(J)$ tends to a constant. From the numerical data we find that

$$E_0 P_0^2 \frac{\mathrm{d}\omega_0}{\mathrm{d}J}\bigg|_{J=0} \approx 0.985 \times 4\pi^2. \tag{3.28}$$

This is within 2% of the value predicted using the rod model.

To compare the rod and Skyrme-Faddeev models over a range of values of J we must choose values for A and C. We will take

$$(4\pi)^2 AC = 1.1, \quad \frac{A}{C} = 3.5. \tag{3.29}$$

The quantity $(4\pi)^2 AC$ has the dimension of energy squared, and its value has been chosen to fit the data for the infinite string. The quantity A/C has the dimension of length to the power of minus two. Its value has been chosen to give a reasonable fit for both the infinite string and for the solitons discussed below . The functions $E_0(J)$, $P_0(J)$ and $\omega_0(J)$ in the rod model have been plotted in figure 1 alongside those for the Skyrme-Faddeev model. It can be seen that the curves for $E_0(J)$ are in excellent agreement; the curves for ω_0 and P_0 are reasonably close for small J, but less close for large values of J.

A final remark concerns the limiting value of ω. Previously we showed that the Faddeev-Skyrme pseudo-energy is unbounded below for $\omega \geq 1$, suggesting that the pseudo-energy does not have critical points for $\omega \geq 1$. Our numerical results for infinite strings confirm that the range of ω is bounded, however, the maximum value is around 1.4, and exceeds the expected value of 1. Thus for $1 \leq \omega \leq 1.4$ the pseudo-energy has critical points, despite being unbounded from below.

3.3 Solitons

Now let us consider the effect of isospin on elastic rods in $\mathbb{R}^3$. Suppose that $(\mathbf{x}_0, \mathbf{m}_0)$ is a critical point of $F_{\omega=0} = V$ and that $V(\mathbf{x}_0, \mathbf{m}_0) = V_0$. The moment of inertia Λ_0 for this critical point may be determined by means of a virial theorem: the energy of a rescaled configuration $(\lambda \mathbf{x}_0, \mathbf{m}_0)$ is

$$V(\lambda \mathbf{x}_0, \mathbf{m}_0) = \lambda \int_\Upsilon A \mathrm{d}s_0 + \frac{1}{\lambda} \int_\Upsilon \left(B\kappa_0^2 + C(\mathbf{t}_0 \cdot \mathbf{m}_0 \times \partial_s \mathbf{m}_0)^2 \right) \mathrm{d}s_0. \tag{3.30}$$

Since $(\mathbf{x}_0, \mathbf{m}_0)$ is a critical point the derivative of the left hand side with respect to λ must evaluate to zero at $\lambda = 1$, so the two integrals on the right hand side of the equation must be equal. It follows that

$$\Lambda_0 = \frac{C}{A} V_0. \tag{3.31}$$

Since F_ω is related to F_0 by equation (3.15) there exists a corresponding critical point $(\mathbf{x}_0/\sqrt{1-\omega^2 C/A}, \mathbf{m}_0)$ of F_ω, and indeed all critical points of F_ω are so obtained. The value of F_ω at the critical point may be deduced from equation (3.15) to be

$$F_\omega = \sqrt{1-\omega^2 C/A}\, V_0. \tag{3.32}$$

Since Λ is proportional to the length of $\mathbf{x}(\Upsilon)$, the value of Λ at this critical point is

$$\Lambda = \frac{1}{\sqrt{1-\omega^2 C/A}} \frac{C}{A} V_0. \tag{3.33}$$

It follows that $J = \omega\Lambda$ and $E = F_\omega + \omega^2 \Lambda$ take the values

$$J = \frac{\omega C/A}{\sqrt{1-\omega^2 C/A}} V_0 \quad \text{and} \tag{3.34}$$

$$E = \frac{1}{\sqrt{1-\omega^2 C/A}} V_0 \tag{3.35}$$

$$= \sqrt{V_0^2 + J^2 A/C} \tag{3.36}$$

at the critical point.

The preceding formulae contain useful qualitative information about the solutions to variational problems 1 and 2 in the elastic rod model. Equation (3.32) implies that the values of F_ω at its critical points all scale with ω in the same way. In particular, the global minimum at $\omega = 0$ remains the global minimum of F_ω for all other values of ω. As ω approaches a critical value the moment of inertia, angular momentum, energy and size diverge.

The behaviour of solutions to the second variational problem is similarly uniform: equation (3.36) captures the dependence of the critical values of E_J on J. The global minimum at $J = 0$ remains the global minimum for all values of J, because the right hand side of (3.36) is monotonic in V_0. At large values of J the energy, moment of inertia and size grow linearly with J, while ω tends to a finite constant. Similar behaviour should be expected from solitons in the Faddeev-Skyrme model.

4 Numerical results

In this section the results of numerical simulations of the Faddeev-Skyrme model will be presented. Local minima of the pseudo-energy functional $F_\omega(\psi)$ have been found for a range of values of the Hopf degree Q and of ω. The majority of simulations were carried out with $\mu = 2$. This choice guarantees that $\omega_1 < \omega_2$, and thus allows us to investigate the possibility that solitons become unstable to processes other than pion decay. Other values of μ were also investigated with Hopf degrees one, two and three.

The numerical algorithm employed was similar to that used in [8]. A simple forward differencing scheme was used on a cubic lattice with a lattice spacing $\Delta x = 0.1$ on a grid typically containing $(240)^3$ latice points. Well-chosen initial configurations were evolved using the quasi-Newton BFGS method to minimize the pseudoenergy functional $F_\omega(\psi)$. Simulations were considered to have converged to local minima if the sup norm of the gradient of $F_\omega(\psi)$ was less than $0.01\Delta x^3$.

Each of our simulations began at $\omega = 0$ and proceeded by making small increments in ω. At each value of ω the algorithm was allowed to converge to a local minimum of the pseudo-energy, and this local minimum was then used as the initial configuration for the next value of ω. Initial configurations at $\omega = 0$ were created using Sutcliffe's rational map ansatz [15]. This involves identifying physical space $\mathbb{R}^3$ with the three-sphere $S^3 \subset \mathbb{C}^2$ using a map

$$(Z_1, Z_0) = \left((x_1 + ix_2)\frac{\sin f(r)}{r}, \quad \cos f(r) + ix_3 \frac{\sin f(r)}{r} \right), \tag{4.1}$$

in which $f(r)$ is some monotonic function of $r = \sqrt{x_1^2 + x_2^2 + x_3^2}$ satisfying the boundary conditions $f(0) = \pi,\ f(\infty) = 0$. Initial configurations are given by maps of the form

$$W = \frac{\psi_1 + i\psi_2}{1 + \psi_3} = \frac{Z_1^\alpha Z_0^\beta}{Z_1^a + Z_0^b}, \tag{4.2}$$

with a, b, α, β natural numbers. These maps have Hopf degree $Q = \alpha b + \beta a$, so that an initial configuration with any desired Hopf degree can easily be constructed. The largest value

of ω that we were able to explore was $\omega = 1$, reflecting the fact that the pseudo-energy is unbounded below thereafter. However, the existence of saddle points of F_ω with $\omega > 1$ is not ruled out.

Below we present location curves and energy density isosurfaces for solitons, and graphs of their energies, both as functions of ω and as functions of isospin. As in recent studies [15, 5], the location curves plotted are the tubular preimages of the curve $\psi_3 = -0.90$.

Energy curves obtained from the rod model are plotted alongside those obtained from the numerics, in order to ascertain whether soliton energies follow the expected behaviour. The rod model curves are obtained from equations (3.35) and (3.36). The value of A/C is taken to be 3.5 for all solitons with $\mu = 2$, and for each soliton the value of E_0 is taken to be the soliton energy at $\omega = 0$. In graphs containing energy curves for several solitons, we choose to plot only one or two curves from the rod model, in order to avoid cluttering the graph. Graphs are presented using normalised units of energy in which $\hat{E} = E/(16\pi^2\sqrt{2})$ and $\hat{J} = J/(16\pi^2\sqrt{2})$; with this convention Ward's conjectured lower bound on the energy [16] is $\hat{E} \geq Q^{3/4}$.

In the previous section it was argued using the elastic rod approximation that the sizes and energies of solitons should scale in a uniform way both with ω and with the isospin J. These predictions are expected to hold for relatively small values of ω or J, but at larger values some deviation from this approximation should be expected. It is well-known that for most values of Q the Faddeev-Skyrme energy has several local minima with similar energies. Thus it is plausible that at large values of J or ω small deviations from the elastic rod approximation can occasionally result in the crossing of energy curves, and hence in a change in the qualitative features of the global minimizer of energy. The results presented below confirm that the $E(\omega)$ curves follow the predictions of the rod model at small ω. Somewhat surprisingly, the $E(J)$ curves continue to do so even at large J. We also observe occasional crossings in both the $E(J)$ and the $E(\omega)$ curves.

4.1 Degrees one, two and three

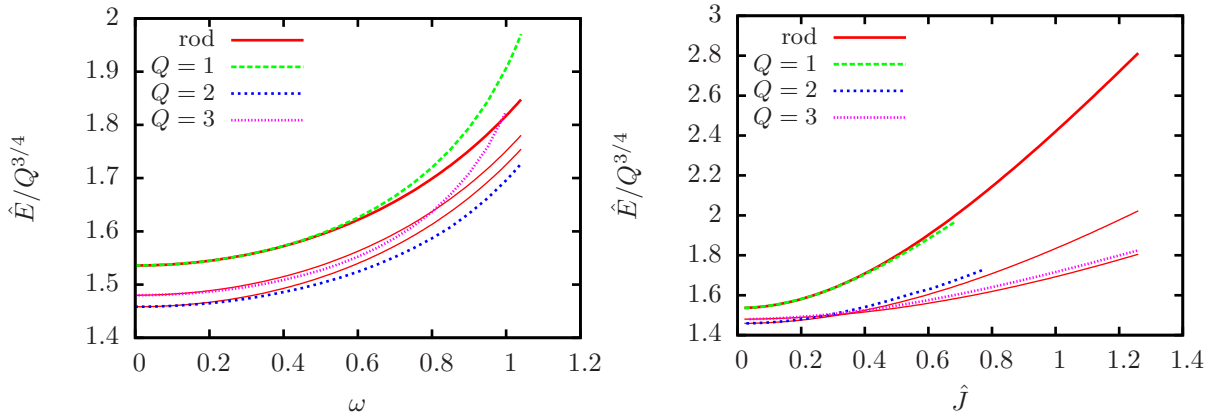

Figure 2: Energy (in units of $Q^{3/4}$) as a function of angular frequency ω and as a function of isospin J for solitons with $Q = 1, 2, 3$ and $\mu = 2$, and energy curves derived within the rod model.

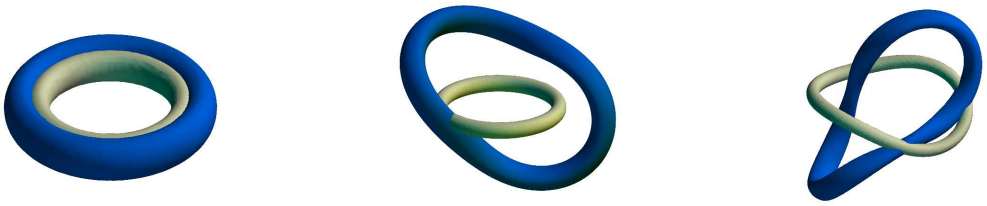

$1\mathcal{A}_{1,1}$ $2\mathcal{A}_{2,1}$ $3\tilde{\mathcal{A}}_{3,1}$

Figure 3: Position curves for solitons with charges $1 \leq Q \leq 3$ at $\mu = 1$. The light green and blue position curves correspond to $\omega = 0$ and $\omega = 1$, respectively.

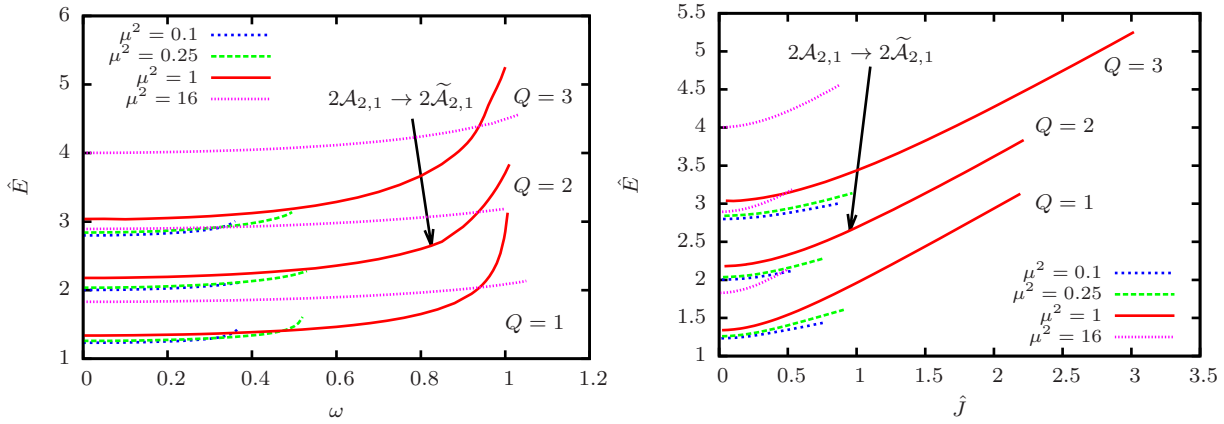

Figure 4: Energy as a function of angular frequency ω and as a function of isospin J for $Q = 1, 2, 3$ for a range of values of μ. The transition $2\mathcal{A}_{2,1} \to \widetilde{\mathcal{A}}_{2,1}$ at $\mu = 1$ and $\omega = 0.86$, is labelled.

For Hopf degrees 1, 2 and 3 simulations were carried out with a range of values of μ. The energy curves for $\mu = 2$ are plotted in figure 2 alongside the predictions from the rod model. These clearly show that the soliton energies scale as expected.

In figure 4 soliton energy curves for a range of values of μ are plotted. Figure 3 shows the soliton location curves for $\mu = 1$ at $\omega = 0$ and $\omega = 1$. For most values of ω and μ the preferred configurations are of type $\mathcal{A}_{1,1}$, $2\mathcal{A}_{2,1}$ and $3\widetilde{\mathcal{A}}_{3,1}$, as in the static case. Here, and in the sequel, we are using the notation introduced by Sutcliffe to label Hopf soliton shapes [15]. Briefly, $Q\mathcal{A}_{n,m}$ denotes an axially symmetric hopfion of charge Q, where the position curve (preimage of $-\psi_\infty$) is a circle, and the preimage of a regular value close to $-\psi_\infty$ is a disjoint union of m closed curves, each winding n times around the circle. In fact $Q = nm$, so including Q in the label is redundant, but convenient. A soliton of type $Q\widetilde{\mathcal{A}}_{n,m}$ has the same qualitative form, but with axial symmetry weakly broken, so the position curve is not exactly circular. Later we will encounter solitons whose position curves are links of two components. These will be denoted $Q\mathcal{L}^{a,b}_{p,q}$ where the subscripts denote the Hopf charges of each component, and the superscripts denote the extra Hopf degree of each component due to its linking with the

other component. Again, we include Q, though this is redundant (since $Q = p + q + a + b$). We will also encounter hopfions whose position curves are torus knots of type (a, b) (where a and b denote the windings of the curve around the S^1 factors in T^2). We denote these $Q\mathcal{K}_{a,b}$

When $Q = 2$, $\mu = 1$ and $\omega \geq 0.86$, our algorithm converges to a buckled $2\widetilde{\mathcal{A}}_{2,1}$ rather than an axial $2\mathcal{A}_{2,1}$ configuration. This configuration did not appear in the earlier study [1], whose attention was restricted to axial symmetry. The buckled configuration seems to be a local minimum of the pseudo-energy, so should be orbitally stable (as explained in section 2). It is likely that an axial $2\mathcal{A}_{2,1}$ configuration continues to exist above $\omega = 0.86$, albeit as a saddle point rather than a minimum of F_ω. Since our algorithm only finds local minima and not saddle points we are unable to determine whether the $2\widetilde{\mathcal{A}}_{2,1}$ has a greater or smaller energy than the $2\mathcal{A}_{2,1}$ for any given value of ω or J.

When $\mu < 1$ our simulations terminate at $\omega = \mu$, as expected. When $\mu > 1$ our algorithm ceases to find any critical points when $\omega = 1$ (although in a few cases it is possible to go slightly beyond $\omega = 1$). This is again consistent with our expectations, as the pseudo-energy is not bounded from below when $\omega > 1$. However, the existence of solutions with $\omega > 1$ is not ruled out, as they may continue to exist as saddle points of the pseudo-energy.

The borderline case $\mu = 1$ is particularly interesting: the graphs of $E(\omega)$ grow rapidly as ω approaches 1. The rod model predicted that soliton energies would diverge at some finite value of ω, and our numerical results suggest that for $\mu = 1$ this value is very close to 1.

4.2 Degree four

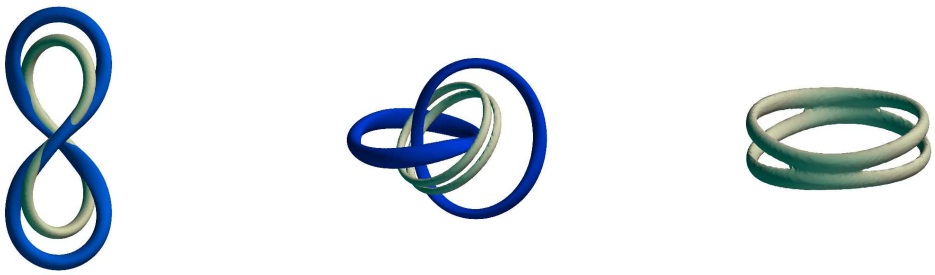

$4\tilde{\mathcal{A}}_{4,1}$ $4\mathcal{A}_{2,2}/4\mathcal{L}^{1,1}_{1,1}$ saddle

Figure 5: Position curves for solitons with $Q = 4$ and $\mu = 2$. In the left and middle pictures the light green and blue position curves correspond to $\omega = 0$ and $\omega = 1$ respectively. The right picture is an intermediate state between $4\mathcal{A}_{2,2}$ and $4\mathcal{L}^{1,1}_{1,1}$ at $\omega = 0.58$.

At degree 4 we have been able to find configurations of types $4\mathcal{A}_{2,2}$, $4\tilde{\mathcal{A}}_{4,1}$ and $4\mathcal{L}^{1,1}_{1,1}$; these are depicted in figure 5. The $4\mathcal{A}_{2,2}$ is axially symmetric and may be thought of as two adjacent $2\mathcal{A}_{2,1}$ solitons. The position curve of the $4\mathcal{A}_{2,2}$ in our model consists of two adjacent circles, whereas in the massless Faddeev-Skyrme model it is a single circle.

The graphs of energy as a function of ω or J are shown in figure 6. The $4\tilde{\mathcal{A}}_{4,1}$ configuration exists for all values of ω in the range [0,1], but the $4\mathcal{A}_{2,2}$ and $4\mathcal{L}^{1,1}_{1,1}$ configurations could only be found in the ranges [0,0.65] and [0.57,1] respectively. At $\omega = 0.57$ the $4\mathcal{A}_{2,2}$ and $4\mathcal{L}^{1,1}_{1,1}$

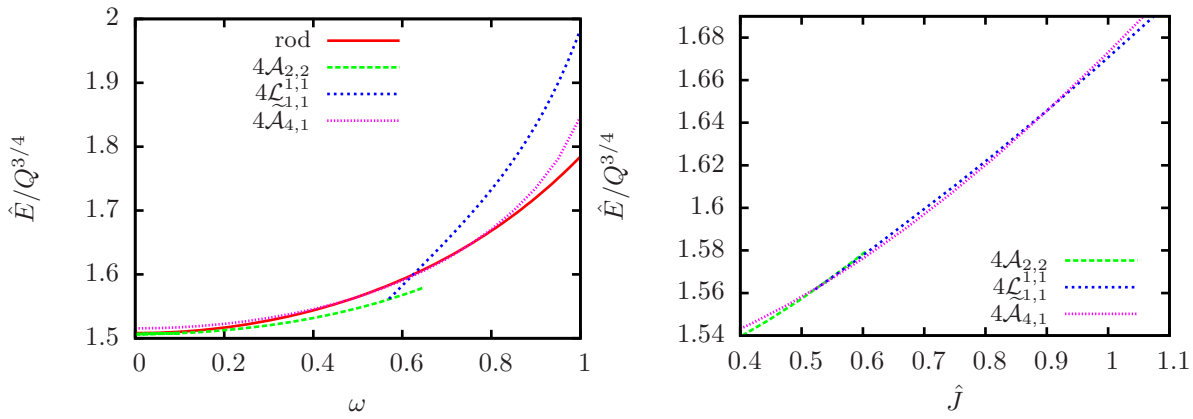

Figure 6: Energy as function of the parameter ω and as a function of isospin J for solitons with $Q = 4$ and $\mu = 2$. In the right panel we only present data in the range $0.4 \leq \hat{J} \leq 1.1$ to better illustrate the energy crossings.

configurations are degenerate in both energy and pseudo-energy, from which we infer that the $4\mathcal{A}_{2,2}$ critical point undergoes a bifurcation at this point. We were also able to find a configuration which seems to be a saddle point of the pseudo-energy at $\omega = 0.58$, suggesting that the bifurcation is a pitchfork bifurcation. This saddle is illustrated in figure 5 but its energy has not been plotted.

When $\omega > 0.65$ our algorithm is unable to find the $4\mathcal{A}_{2,2}$ and instead converges to the $4\mathcal{L}^{1,1}_{1,1}$. Since the $4\mathcal{A}_{2,2}$ configuration is axially symmetric it is likely to continue to exist as a critical point of the pseudo-energy beyond $\omega = 0.65$; the most likely reason for our code's failure to find it is that is a saddle point rather than a local minimum.

Both the $E(\omega)$ and the $E(J)$ graphs exhibit crossings. The minimum of the energy at $\hat{J} = 0$ is the $4\mathcal{A}_{2,2}$ configuration. All three energy graphs cross in the range $0.5 \leq \hat{J} \leq 1.0$, and for $\hat{J} \geq 1.0$ the energy-minimzer is the $4\mathcal{L}^{1,1}_{1,1}$ link. It is likely that the energy-minimizer for fixed ω is always the $4\mathcal{A}_{2,2}$, but for $\omega \geq 0.65$ it is difficult to be sure of this without being able to construct the $4\mathcal{A}_{2,2}$ configuration. We note that, despite the presence of crossings, the energy curves generally follow the rod model predictions, the only significant deviant being the $E(\omega)$ curve for the link when $\omega > 0.6$.

4.3 Degrees five to eight

At degree five we found two distinct local minima of the pseudo-energy, namely a $5\mathcal{L}^{1,2}_{1,1}$ link and a $5\widetilde{\mathcal{A}}_{5,1}$ buckled ring, see figure 7. When $\omega = 0$ the link has the lower energy. The two curves for $E(\omega)$ cross when $\omega = 0.82$ and thereafter the ring has the lower energy. In contrast, the $E(J)$ curves for these configurations do not cross and the link has the lower energy for any given value of J.

At degree six we again found two distinct local minima of the pseudo-energy. These were links of type $6\mathcal{L}^{1,1}_{2,2}$ and $6\mathcal{L}^{1,1}_{3,1}$, shown in figure 8. Unlike the study [5], we did not find a $6\mathcal{A}_{3,2}$ configuration; this could be due to a different choice of potential function or a different choice of the mass parameter μ. The $6\mathcal{L}^{1,1}_{2,2}$ link has a lower energy than the $6\mathcal{L}^{1,1}_{3,1}$ link for all values

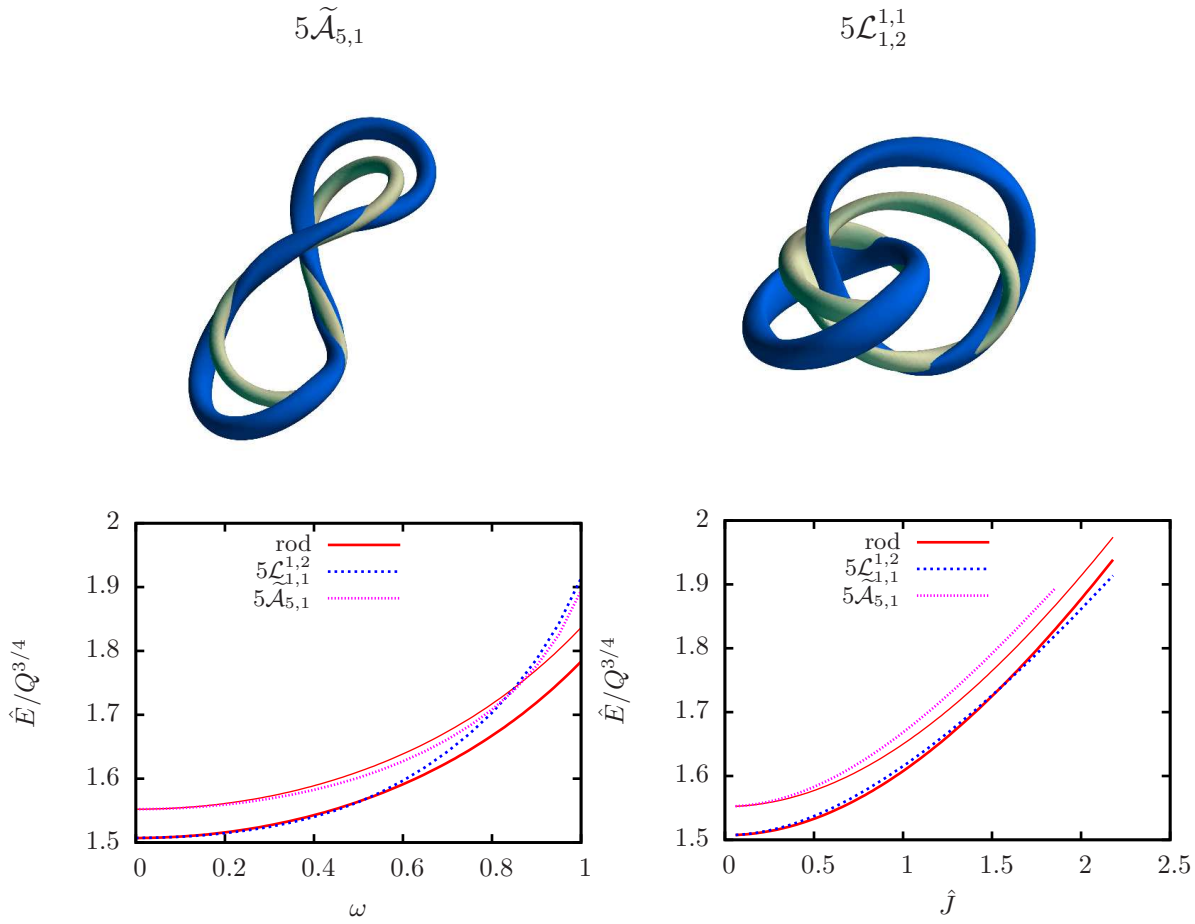

Figure 7: Solitons with $Q = 5$ and $\mu = 2$. Top row: position curves for the $5\widetilde{\mathcal{A}}_{5,1}$ and $5\mathcal{L}^{1,1}_{1,2}$ configurations, with light green and blue position curves corresponding to $\omega = 0$ and $\omega = 1$ respectively. Bottom row: energy as function of the parameter ω and as a function of isospin J.

of ω and for all values of J.

At degree seven the only minimum of the pseudo-energy found was a $7\mathcal{K}_{3,2}$ knot, and this is shown in figure 9.

At degree eight the three energy minima found were a link of type $8\mathcal{L}^{1,1}_{3,3}$ and a knot of type $8\mathcal{K}_{3,2}$, see figure 10. We did not find a soliton corresponding to the $8\mathcal{A}_{4,2}$ configuration in [5]. Within the limits of numerical accuracy the $8\mathcal{L}^{1,1}_{3,3}$ and $8\mathcal{K}_{3,2}$ configurations are degenerate in energy when $\omega = 0$. As ω increases the knot energy grows faster than that of the link, so that the link has the lower energy. When ω reaches the value 0.38 the link collapses to the knot, which has a smaller pseudo-energy. Our algorithm is unable to find the link at larger values of ω. It is likely that when $\omega \geq 0.38$ the link is an unstable critical point of the pseudo-energy, and that it continues to have a lower energy than the knot. As far as we can tell, the $E(J)$ curves for the two solitons coincide, at least within the range of values of J in which both can be constructed. Note that, since their energies are indistinguishable at $\omega = 0$, this is precisely what the rod model predicts.

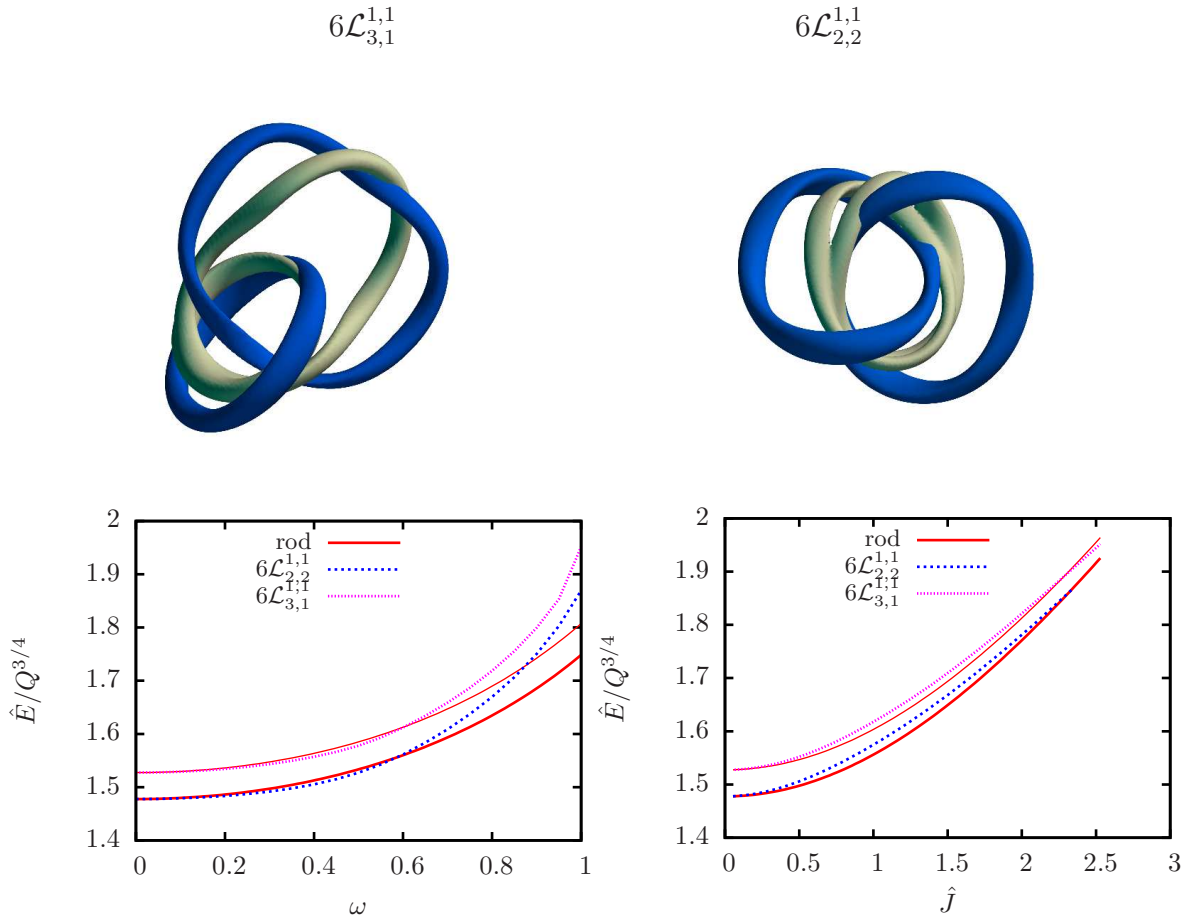

Figure 8: Solitons with $Q = 6$ and $\mu = 2$. Top row: position curves for the $6\mathcal{L}^{1,1}_{2,2}$ and $6\mathcal{L}^{1,1}_{3,1}$ configurations, with light green and blue position curves corresponding to $\omega = 0$ and $\omega = 1$ respectively. Bottom row: energy as function of the parameter ω and as a function of isospin J.

5 Conclusions

To summarize, we have reformulated the problem of constructing internally spinning Hopf solitons of frequency ω as a variational problem for pseudoenergy F_ω, and solved this problem numerically for Hopf charges 1–8, $0 \leq \omega \leq 1$ without imposing any spatial symmetries. For each local minimizer of the static energy F_0 we have constructed a curve of isospinning hopfions, parametrized by ω, for which the total energy $E(\omega)$ and conserved isospin $J(\omega)$ were calculated. Generically, the solitons persist for all $\omega \leq \min\{1, \mu\}$, where μ is the meson mass of the model, and their qualitative shape is independent of ω. We noted two exceptions to this: for $Q = 2$, $\mu = 1$, the solitons undergo a bifurcation as ω increases through 0.86, branching from $2\mathcal{A}_{2,1}$ to $2\widetilde{\mathcal{A}}_{2,1}$ (i.e. they lose axial symmetry); for $Q = 4$, $\mu = 2$, the axially symmetric $4\mathcal{A}_{2,2}$ soliton branches to a link $4\mathcal{L}^{1,1}_{1,1}$ as ω increases through 0.58. Even when no such bifurcation occurs, the shape of the lowest energy soliton with fixed ω can change as ω varies, because the graphs of $E(\omega)$ for different solitons with the same Hopf degree can cross.

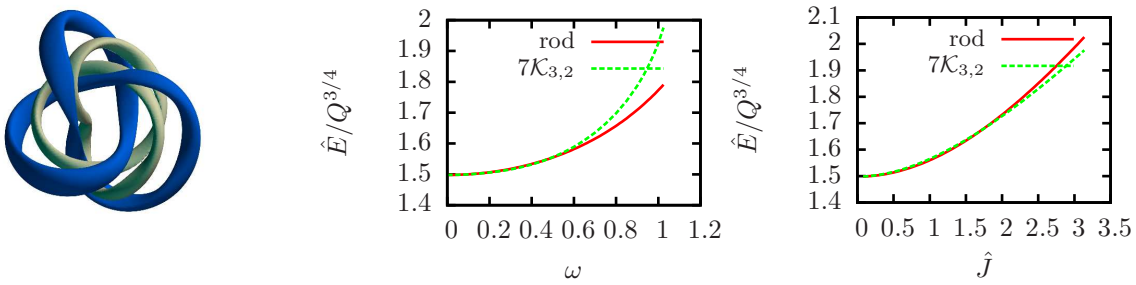

Figure 9: Solitons with $Q = 7$ and $\mu = 2$. The light green and blue curves in the left figure are position curves for solitons at $\omega = 0$ and $\omega = 1$ respectively. The two graphs show energy as a function of the parameter ω and as a function of isospin J.

We found that this happens for $Q = 5$, $\mu = 2$, for example. Similarly, the shape of the lowest energy soliton with fixed isospin J can change as J varies, if the graphs of $E(J)$ for different soliton branches cross, as happens, for example for $Q = 4$, $\mu = 2$. Such crossings seem to be comparatively rare, however.

We have developed a time-dependent extension of the the elastic rod model of Hopf solitons, which predicts simple, uniform scaling behaviour of the total energy and isospin of hopfions as ω varies, namely

$$E(\omega) = \frac{E_0}{\sqrt{1-(\omega/\omega_*)^2}}, \qquad J(\omega) = \frac{(\omega/\omega_*^2)E_0}{\sqrt{1-(\omega/\omega_*)^2}} \tag{5.1}$$

where E_0 is the static soliton energy and ω_* is an (unknown) parameter, depending only on the details of the Faddeev-Skyrme model under consideration (but independent of Q, and of which branch of local minimizers one is following). Despite having only one free parameter, the rod model fits the $E(\omega)$ graphs well for small ω, and the $E(J)$ graphs well for all J. The rod model predicts that the energy graphs never cross, and that solitons never change shape (they just dilate uniformly), as ω (or J) varies which, again, is in good qualitative agreement with our numerical results.

Acknowledgments

This work was financially supported by the UK Engineering and Physical Sciences Research Council (grant number EP/G009678/1). Some of the work of JJ was undertaken at the University of Antwerp, Belgium, financially supported by an FWO Visiting Post-Doctoral Fellowship, and some of the work of DH was carried out at Durham University, supported by the Engineering and Physical Sciences Research Council (grant number EP/G038775/1). Most numerical calculations were performed on the ARC1 HPC system at the University of Leeds, some on the cluster SKIF at the Belarusian State University. We would like to thank Paul Sutcliffe, Steffen Krusch, David Foster, Alexey Halawanau and Joan Camps for helpful discussions.

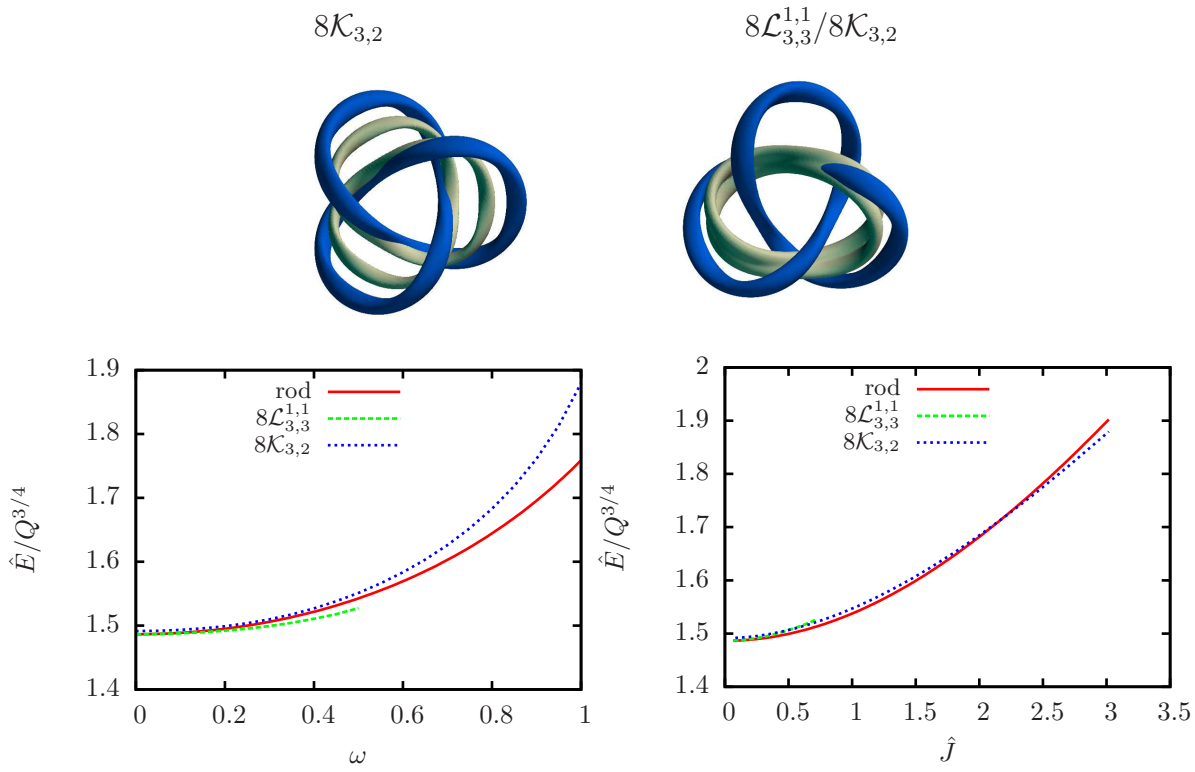

Figure 10: Solitons with $Q = 8$ and $\mu = 2$. The top row shows position curves at $\omega = 0$ (light green) and $\omega = 1$ (blue). The bottom row shows energy as a function of the parameter ω and as a function of isospin J.

References

[1] A. Acus, A. Halavanau, E. Norvaisas and Y. Shnir, "Hopfion canonical quantization," Phys. Lett. B **711** (2012) 212.

[2] G.S. Adkins, C.R. Nappi and E. Witten, "Static properties of nucleons in the Skyrme model" *Nucl. Phys.* **B228** (1983) 552.

[3] R.A. Battye, S. Krusch and P.M. Sutcliffe, "Spinning Skyrmions and the Skyrme Parameters" *Phys. Lett.* **B626** (2005) 120.

[4] L. D. Faddeev and A. J. Niemi, "Knots and particles" *Nature* **387** (1997) 58.

[5] D. Foster, "Massive Hopfions" *Phys. Rev.* **D83** (2011) 085026.

[6] D. Harland and D. Foster, "Helical buckling of Skyrme-Faddeev solitons," *Proc. R. Soc. A* **468** (2012) 3172.

[7] D. Harland, J.M. Speight and P.M. Sutcliffe, "Hopf solitons and elastic rods" *Phys. Rev.* **D83** (2011) 065008.

[8] J. Jäykkä and J.M. Speight, "Supercurrent coupling destabilizes knot solitons," *Phys. Rev. D* **84**, 125035 (2011).

[9] D.J. Jee, "Gauss-Bonnet formula for general Lorentzian surfaces," *Geometriae Dedicata* **15** (1984) 215.

[10] S. Krusch and J.M. Speight, "Fermionic quantization of Hopf solitons" *Commun. Math. Phys.* **264** (2006) 391.

[11] R.A. Leese, N.S. Manton and B.J. Schroers, "Attractive channel Skyrmions and the deuteron" *Nucl. Phys.* **B442** (1995) 228.

[12] F. Lin and Y. Yang, "Existence of energy minimizers as stable knotted solitons in the Faddeev model" *Commun. Math. Phys.* **249** (2004) 273.

[13] R.S. Palais, "The principle of symmetric criticality" *Commun. Math. Phys.* **69** (1979) 19.

[14] B.J. Schroers, "Dynamics of moving and spinning Skyrmions" *Z. Phys.* **C61** (1994) 479.

[15] P. Sutcliffe, "Knots in the Skyrme-Faddeev model," *Proc. Roy. Soc. Lond. A* **463** (2007) 3001.

[16] R.S. Ward, "Hopf solitons on S^3 and $\mathbb{R}^3$," *Nonlinearity* **12** (1999) 241–246.